Front. Earth Sci. 2013, 7(2): 227–237
DOI 10.1007/s11707-013-0354-2

RESEARCH ARTICLE

Combining BPANN and wavelet analysis to simulate hydro-climatic processes——a case study of the Kaidu River, North-west China

Jianhua XU (✉)[1], Yaning CHEN[2], Weihong LI[2], Paul Y. PENG[3], Yang YANG[1], Chunan SONG[1], Chunmeng WEI[1], Yulian HONG[1]

1 The Key Laboratory of GIScience of the Education Ministry of China, The Research Center for East-West Cooperation in China, East China Normal University, Shanghai 200241, China
2 The Key Laboratory of Oasis Ecology and Desert Environment, Xinjiang Institute of Ecology and Geography, Chinese Academy of Sciences, Urumqi 830011, China
3 Department of Community Health and Epidemiology, Queen's University, Kingston, K7L 3N6, Canada

Abstract Using the hydrological and meteorological data in the Kaidu River Basin during 1957–2008, we simulated the hydro-climatic process by back-propagation artificial neural network (BPANN) based on wavelet analysis (WA), and then compared the simulated results with those from a multiple linear regression (MLR). The results show that the variation of runoff responded to regional climate change. The annual runoff (AR) was mainly affected by annual average temperature (AAT) and annual precipitation (AP), which revealed different variation patterns at five time scales. At the time scale of 32-years, AR presented a monotonically increasing trend with the similar trend of AAT and AP. But at the 2-year, 4-year, 8-year, and 16-year time-scale, AR presented non-linear variation with fluctuations of AAT and AP. Both MLR and BPANN successfully simulated the hydro-climatic process based on WA at each time scale, but the simulated effect from BPANN is better than that from MLR.

Keywords hydro-climatic process, Kaidu River, simulation, wavelet analysis (WA), back-propagation artificial neural network (BPANN), multiple linear regression (MLR)

1 Introduction

Water shortages and related ecological degradation are the most pressing environmental issues in northwestern China. To establish proper water management strategies, thoroughly understanding the mechanism of the hydro-climatic process is important (Xu et al., 2010).

In the past 20 years, many studies have been conducted to evaluate climate change and hydrological processes in northwestern China (Chen and Xu, 2005; Wang et al., 2010; Zhang et al. 2010). A number of studies indicated that there was a visible transition in the hydro-climatic processes during the past half-century (Chen et al., 2006; Shi et al., 2007; Hao et al., 2008), which was characterized by a continual increase in temperature and precipitation, added river runoff volumes, increased lake water surface elevation and area, and elevated groundwater levels. However, such inquiries may be designed to determine if these changes represent a localized transition to a warm and wet climate type in response to global warming, or merely reflect a centennial periodicity in hydrological dynamics.

Theoretically, a hydro-climatic process can be evaluated to determine if it is in an ordered, deterministic system, an unordered, random system, or a chaotic, dynamic system, and whether change patterns of periodicity or quasi-periodicity exist. However, it is difficult to achieve a thorough understanding of the complex mechanism of a hydro-climatic process (Cannon and McKendry, 2002). Specifically, effective means have not been discovered to thoroughly understand the dynamics of hydro-climatic process at different time scales (Xu et al., 2008a; Xu et al., 2013). Therefore, more studies are required to explore the hydro-climatic process from different perspectives and using different methods (Xu et al., 2009a, b). Specific to the Kaidu River, a question of interest will be the variation patterns of the hydro-climatic process at different time

Received October 18, 2012; accepted December 13, 2012

E-mail: jhxu@geo.ecnu.edu.cn

scales. To date, this question has not been answered satisfactorily (Xu et al., 2010, 2011a).

Using the data series from the hydrological and meteorological stations in the Kaidu River Basin of northwestern China, this study simulated the annual runoff (AR) with its related regional climatic factors at different time scales by back-propagation artificial neural network (BPANN) based on wavelet analysis (WA), then compared the simulated results with those from multiple linear regression (MLR).

2 Study area and data

2.1 Study area

The Kaidu River is situated at the north fringe of the Yanqi Basin on the south slope of the Tianshan Mountains in Xinjiang, China, and is enclosed between latitudes 42°14′–43°21′N and longitudes 82°58′–86°05′E (Fig. 1). The river starts from the Hargat Valley and the Jacsta Valley in Sarming Mountain with a maximum altitude of 5000 m (the middle part of the Tianshan Mountains), and ends in Bosten Lake, which is located in the Bohu County of Xinjiang. This lake is the biggest lake in Xinjiang (also once the biggest interior fresh water lake in China) and immediately starts another river known as the Kongque River. The catchment area of the Kaidu River above Dashankou, is 18827 km^2, with an average elevation of 3100 m (Tao et al., 2007).

Bayinbuluke wetland, which is in the Kaidu River Basin, is the largest wetland of the Tianshan Mountain area. The large areas of grassland and marshes in the Bayanbuluke wetland have provided favorable conditions for swan survival and reproduction. For this reason, it became China's sole state-level swan nature reserve. The annual average temperature (AAT) is only −4.6°C and the extreme minimum temperature is −48.1°C. The snow cover days are as many as 139.3 d and the largest average snow depth is 12 cm. As the unique high alpine cold climate and topography, it cultivates various alpine grassland and meadow ecosystems, having abundant aquatic plants, animals and good grassland resources. It is the birthplace and water saving place of the Kaidu River and plays a crucial role in regulating water, reserving water, and maintaining water balance. It also plays the utmost important role in protecting the Bosten Lake, its surrounding wetlands, and the ecological environment and green corridor of the lower reaches of Tarim River.

2.2 Data

Some studies have shown that the river's runoff is influenced by exogenous variables such as matter and energy, which are not constant (Chen and Kumar, 2004; Shao et al., 2009). For the Kaidu River, it is an inland river, and its stream flow mainly comes from a mountainous area, i.e., the Tianshan Mountains. In other words, the runoff of the Kaidu River is mainly fed by precipitation and snowmelt in the Tianshan Mountains. Therefore, the climatic factors, especially temperature and precipitation, directly affect the annual changes in the runoff. So we use the runoff, temperature, and precipitation data to analyze the hydro-climatic process in the Kaidu River. The runoff data were from the Dashankou hydrological station, and temperature and precipitation data were from the Bayinbuluke meteorological station. The two stations are located in the mountain areas where the amount of water used by humans is negligible compared to the total discharge.

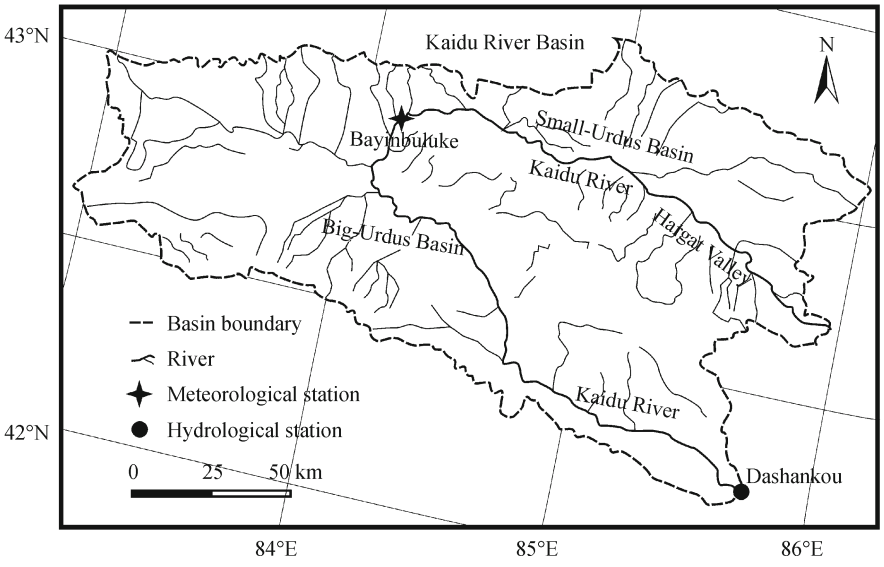

Fig. 1 Location of the study area

Therefore, it was assumed that the observed data reflect the natural conditions (Chen et al., 2012).

Long-term climate changes can alter the runoff production pattern, the timing of hydrological events, and the frequency and severity of floods, particularly in arid or semi-arid regions. A small change in precipitation and temperature may result in marked changes in runoff (Gan, 2000). To investigate the runoff and its related climatic effect, this study used the time series data of AR, AAT, and annual precipitation (AP) from 1957 to 2008.

3 Methods

To reveal the variation of runoff and its response to the regional climate change at different time scales, we conducted a comprehensive study using WA, BPANN, and MLR. First, WA was used to reveal the variation patterns in AR and its related climatic factors at different time scales. Secondly, the relationship between AR and its related climatic factors was simulated by BPANN based on WA at different time scales. Finally, the simulated results from BPANN were compared with those from MLR based on WA.

3.1 Wavelet analysis

Wavelet transformation has been shown to be a powerful technique for characterizing the frequency, intensity, time position, and duration of variations in climate and hydrological time series (Smith et al., 1998; Labat, 2005; Chou, 2007; Xu et al., 2009b). WA can also reveal localized time and frequency information without requiring the time series to be stationary, as required by a Fourier transform and other spectral methods (Torrence and Compo, 1998).

A continuous wavelet function $\Psi(\eta)$ that depends on a nondimensional time parameter η can be written as (Labat, 2005):

$$\Psi(\eta) = \Psi(a,b) = |a|^{-1/2}\Psi\left(\frac{t-b}{a}\right), \tag{1}$$

where, t denotes time, a is the scale parameter and b is the translation parameter. $\Psi(\eta)$ must have a zero mean and be localized in both time and Fourier space (Farge, 1992). The continuous wavelet transform (CWT) of a discrete signal, $x(t)$, such as the time series of runoff, temperature, or precipitation, is expressed by the convolution of $x(t)$ with a scaled and translated $\Psi(\eta)$,

$$W_x(a,b) = |a|^{-1/2}\int_{-\infty}^{+\infty} x(t)\Psi^*\left(\frac{t-b}{a}\right)\mathrm{d}t, \tag{2}$$

where, * indicates the complex conjugate, and $W_x(a, b)$ denotes the wavelet coefficient. Thus, the concept of frequency is replaced by that of scale, which characterizes the variation in the signal, $x(t)$ at a given time scale.

Selecting a proper wavelet function is a prerequisite for time series analysis. The actual criteria for wavelet selection includes self-similarity, compactness, and smoothness (Ramsey, 1999; Xu et al., 2004). For the present study, Symlet 8 was chosen as the wavelet function according to these criteria.

The nonlinear trend of a time series, $x(t)$, can be analyzed at multiple scales through wavelet decomposition on the basis of the discrete wavelet transform (DWT). The DWT is defined taking discrete values of a and b (Banakar and Azeem, 2008). The full DWT for signal, $x(t)$, can be represented as (Mallat, 1989):

$$x(t) = \sum_k \mu_{j_0,k}\phi_{j_0,k}(t) + \sum_{j=1}^{j_0}\sum_k \omega_{j,k}\psi_{j,k}(t), \tag{3}$$

where $\phi_{j_0,k}(t)$ and $\psi_{j,k}(t)$ are the flexing and parallel shift of the basic scaling function, $\phi(t)$, and the mother wavelet function, $\psi(t)$, and $\mu_{j_0,k}(j<j_0)$ and $\omega_{j,k}$ are the scaling coefficients and the wavelet coefficients, respectively. Generally, scales are based on powers of 2, which is the dyadic DWT (Sun et al., 2006).

Once a mother wavelet is selected, the wavelet transform can be used to decompose a signal according to scale, allowing separation of the fine-scale behavior (detail) from the large-scale behavior (approximation) of the signal (Bruce et al., 2002). The relationship between scale and signal behavior is designated as follows: a low scale corresponds to compressed wavelet as well as rapidly changing details, namely high frequency, whereas a high scale corresponds to stretched wavelet and slowly changing coarse features, namely low frequency. Signal decomposition is typically conducted in an iterative fashion using a series of scales such as a = 2,4,8,...,2^L, with successive approximations being split in turn so that one signal is broken down into many lower resolution components.

The wavelet decomposition and reconstruction were used to approximate the nonlinear variation of AR and its related climatic factors over the entire study period at the selected different time scales.

3.2 BPANN based on wavelet analysis

To disclose the relationship between the runoff with its related climatic factors at different time scales, this study employed BPANN based on the results of wavelet decomposition. We first approximated the variation patterns of runoff and its related climate factors, such as AR, ATT, and AP using wavelet decomposition on the basis of the DWT at different time scales. Then the statistical relationship between AR with AAT and AP were revealed by using BPANN based on the wavelet approximation.

In back-propagation networks, a number of smaller processing elements (PEs) are arranged in layers: an input layer, one or more hidden layers, and an output layer (Hsu et al., 1995). The input from each PE in the previous layer (x_i) is multiplied by a connection weight (w_{ji}). These connection weights are adjustable and may be likened to the coefficients in statistical models. At each PE, the weighted input signals are summed and a threshold value (θ_j) is added. This combined input (I_j) is then passed through a nonlinear transfer function ($f(\bullet)$) to produce the output of the PE(y_j). The output of one PE provides the input to the PEs in the next layer. This process can be summarized in Eqs. (4) and (5) and illustrated in Fig. 2 (Maier and Dandy, 1998).

$$I_j = \sum w_{ji} x_i + \theta_j, \tag{4}$$

$$y_i = f(I_j). \tag{5}$$

Our ANN model is a three-tier structure: an input X with two variables (i.e., AAT and AP) is linearly mapped to intermediate variables (called hidden neurons) H, which are then nonlinearly mapped to the output y (i.e., AR).

By comparing the advantages and disadvantages of artificial neural network transfer functions (Dorofki et al., 2012), we selected the activation function as hyperbolic tangent sigmoid transfer function as follows:

$$f(I) = \frac{(1-e^{-I})}{(1+e^{-I})}, \tag{6}$$

where $f(\bullet)$ represents the transfer function, and I represents input.

The purpose of the model is to capture the relationship between a historical set of model inputs and corresponding outputs. As mentioned above, this is achieved by repeatedly presenting examples of the input/output relationship to the model and adjusting the model coefficients (i.e., the connection weights) in an attempt to minimize an error function between the historical outputs and the outputs predicted by the model. This calibration process is generally referred to as 'training'. The aim of the training procedure is to adjust the connection weights until the global minimum in the error surface has been reached. The back-propagation training process is summarized in Fig. 3 (Moghadassi et al., 2009).

The back-propagation process is commenced by presenting the first example of the desired relationship to the network. The input signal flows through the network, producing an output signal, which is a function of the values of the connection weights, the transfer function, and the network geometry. The output signal produced is then compared with the desired (historical) output signal with the aid of an error (cost) function.

The model parameters are optimized by minimizing the mean square error given by the cost function:

$$E = \left\langle ||y - y^{obs}||^2 \right\rangle, \tag{7}$$

where y^{obs} is the observed data, $\langle \bullet \rangle$ denotes a sample or time mean.

Because it can train any network as long as its weight, net input, and transfer functions have derivative functions (Kermani et al., 2005), we selected Levenberg-Marquardt (trainlm) as the training function in the computing environment of MATLAB.

3.3 Wavelet regression analysis

To compare the simulated results from BPANN with those from MLR at different time scales, we also employed the wavelet regression analysis, i.e. regression based on WA. This method fits MLR equation (MLRE) between AR with AAT and AP by using MLR based on the results of wavelet approximation (Xu et al., 2008b; Xu et al., 2011b).

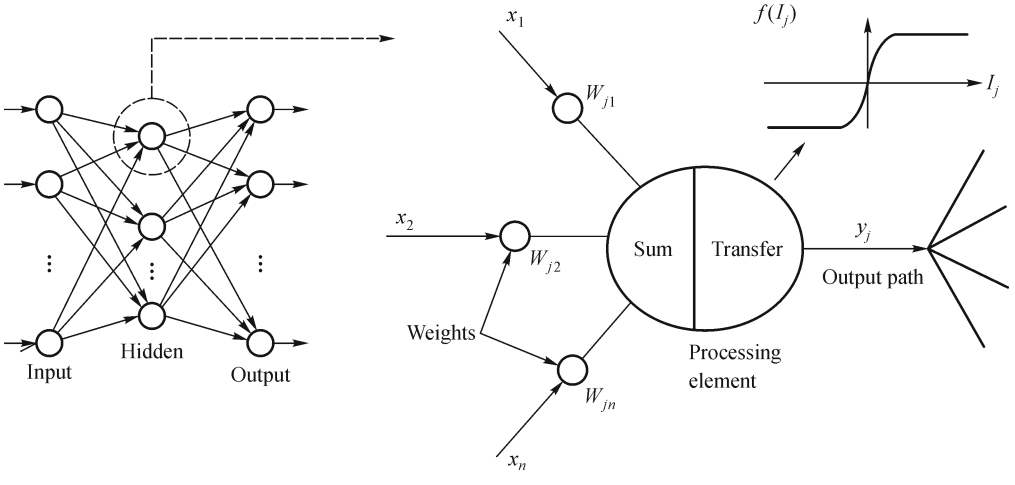

Fig. 2 Operation of a typical back-propagation artificial neural network

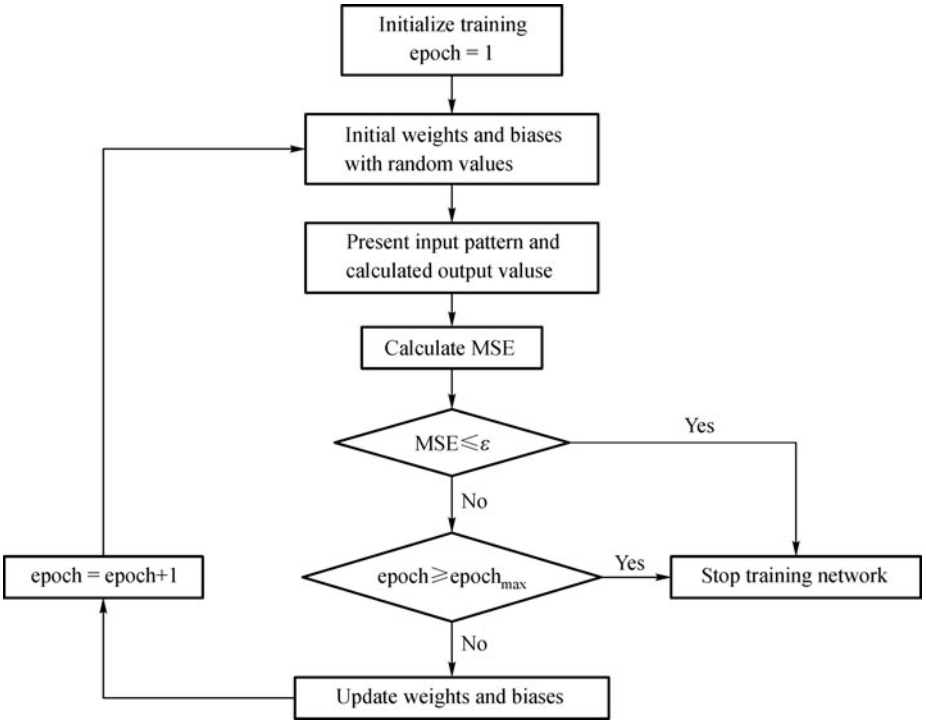

Fig. 3 Back-propagation training process

The MLR model is

$$y = a_0 + a_1x_1 + a_2x_2 + ... + a_ix_i, \tag{8}$$

where, y is the dependent variable, x_i the independent variables, and a_i is the regression coefficient, which is generally calculated by method of least squares (Xu, 2002). In this study, the dependent variable is the AR and the independent variables are related climatic factors, such as the AAT and AP, etc.

3.4 Effect test of estimates

To identify the uncertainty of the estimates for a given timescale, the coefficient of determination was calculated as follows:

$$\mathrm{CD} = 1 - \frac{RSS}{TSS} = 1 - \frac{\sum_{i=1}^{n}(y_i - \hat{y}_i)^2}{\sum_{i=1}^{n}(y_i - \overline{y})^2}, \tag{9}$$

where, CD is the coefficient of determination; $\hat{y}_i$ and y_i are the simulate value and actual data of runoff respectively; $\overline{y}$ is the mean of $y_i(i = 1,2,3,...,n)$; $RSS = \sum_{i=1}^{n}(y_i - \hat{y}_i)^2$ is the residual sum of squares; $TSS = \sum_{i=1}^{n}(y_i - \overline{y})^2$ is the total sum of squares. The coefficient of determination is a measure of how well the simulated results represent the actual data. A bigger coefficient of determination indicates a higher certainty and lower uncertainty of the estimates (Xu, 2002).

To compare the relative goodness between the ANN and MLR fit for a given timescale, we also used the measure of Akaike information criterion (AIC) (Anderson et al., 2000). The formula of *AIC* is as follows:

$$AIC = 2k + n\ln(RSS/n), \tag{10}$$

where k is the number of parameters estimated in the model; n is the number of samples; *RSS* is the same as in Eq.(9). A smaller *AIC* indicates a better model.

For small sample sizes (i.e., $n/k \leqslant 40$), the second-order Akaike Information Criterion (AIC_c) should be used instead

$$AIC_c = AIC + \frac{2k(k+1)}{n-k-1}, \tag{11}$$

where, n is the sample size. As the sample size increases, the last term of the AIC_c approaches zero, and the AIC_c tends to yield the same conclusions as the *AIC* (Burnham and Anderson, 2002).

4 Results

4.1 Climate factors related with runoff

Some studies have shown that stream flows can also be influenced by other variables (called exogenous variables in time series analysis), such as matter and energy, and that such influences might not be constants (Chen and

Kumar, 2004; Shao et al., 2009). The river's flow mainly comes from mountainous watershed, especially in an arid inland river basin (Chen et al., 2009). As one of the headwaters of the Tarim River Basin, the Kaidu River is supplied primarily by the mixed water of snowmelt and precipitation. Therefore, there are conceivably close relationships between runoff and a set of regional climate factors. Our previous study indicated that (Xu et al., 2008b) the AAT and AP are the most important factors related to the AR. The result was also supported by the other studies for the headwaters of the Tarim River Basin (Chen et al., 2006; Tao et al., 2007; Hao et al., 2008).

Figure 4 showed the variation patterns of temperature and precipitation at different time scales. The wavelet decomposition for the time series of AAT and AP at five time scales educed five variation patterns. These five time scales are also designated as S1 to S5, which represent 2-year, 4-year, 8-year, 16-year, and 32-year time scale respectively. There are drastic fluctuations in the curve S1 and S2. The curve S3 is getting smoother and the increasing trend becomes even more obvious as the scale level increases. The curve S4 and S5 show a monotonic increasing trend.

4.2 BPANN simulation for the hydro-climatic process

Accordingly, the variation for the time series of AR was

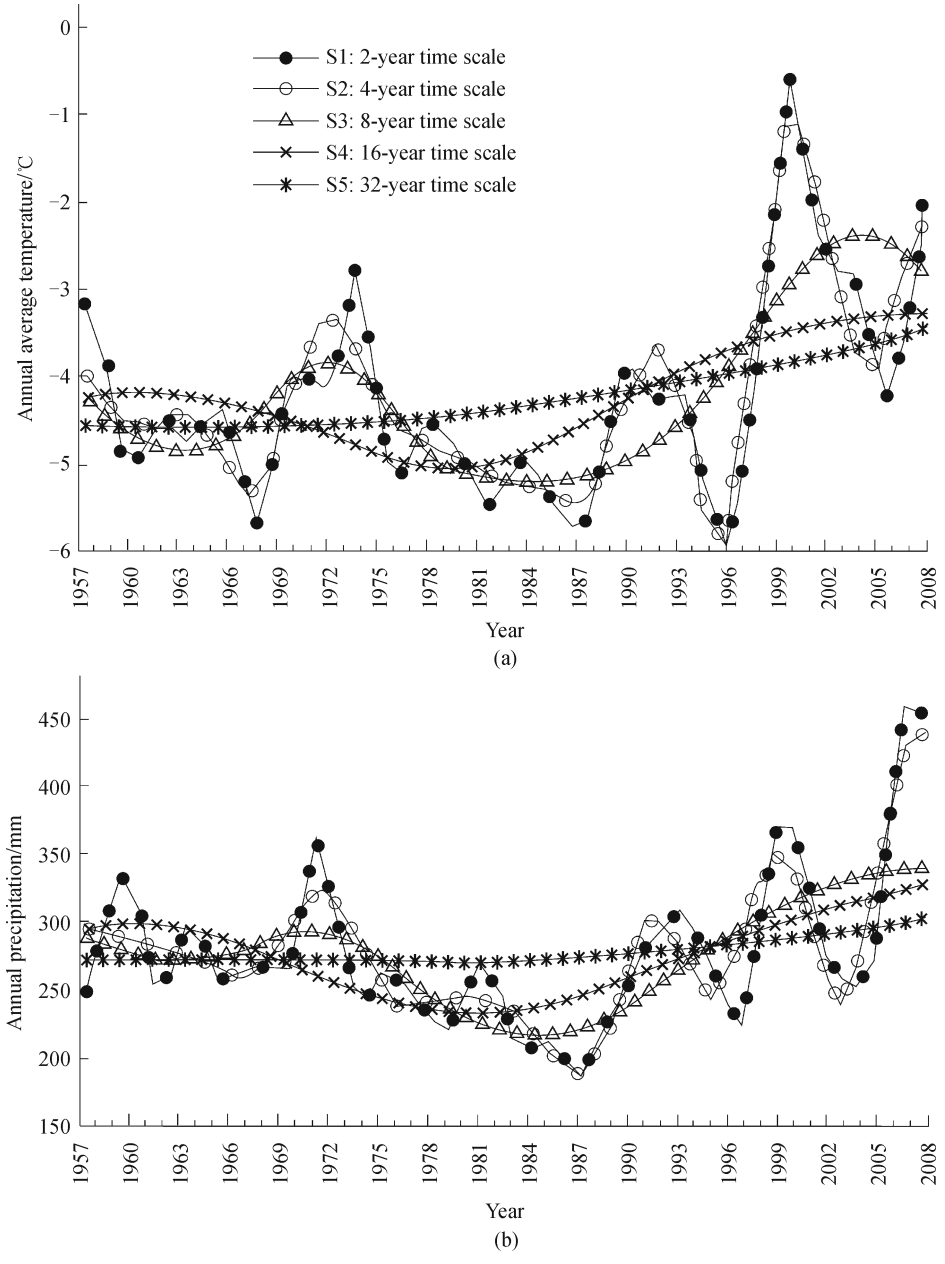

Fig. 4 Variation patterns of AAT (a) and AP (b) at different time scales

analyzed at five time scales through wavelet decomposition on the basis of the DWT. The results also tell us that variation patterns of AR were different at different time scales.

For the purpose of understanding the hydro-climatic process, based on the results of wavelet decomposition at different time scales, the BPANN was employed to simulate the relationship between AR with AAT and AP.

Our study considered a three-layer BPANN, i.e., input layer, output layer and hidden layer, to simulate the nonlinear relationship between AR with AAT, and AP at each time scales. The input layer contains two variables, AAT and AP; the output layer contains one variable, AR; and the neuron number of hidden layers is four. Table 1 shows the optimized parameters for BPANN.

The numerical work was carried out using MATLAB. We selected tansig as the transfer function, and trainlm as the training function to train the network.

Based on wavelet decomposition results of AR, AAT, and AP from 1957 to 2008, we randomly extracted 80%, 10%, and 10% of the data as training, validation, and testing samples, respectively. The results show that, at the time scales of S1–S5 (i.e., 2-year, 4-year, 8-year, 16-year, and 32-year), all network models have reached the expected error target (0.001) with learning rate of 0.01. The optimized parameters of the BPANN for the hydro-climatic process at different time scales are showed in Table 1.

Table 1 reveals that, as the time scale increased from S1 to S5, the estimated error decreases. The average absolute error and relative error for the simulation of AR at time scale of S1 are $2.3163 \times 10^8 m^3$ and 6.65%, respectively, but those at time scale of S5 only are $0.0617 \times 10^8 m^3$ and 0.18%, respectively.

The coefficient of determination and AIC value for BPANN (in Sect. 4.3.2 also show that the simulated effect at a larger time scale is better than that at a smaller time scale.

4.3 Comparison between BPANN and MLR

4.3.1 Regression model

To compare the simulated results from BPANN with those from the regression model, a group of multiple linear regression equations (MLREs) were fitted based on the results of wavelet decomposition at different time scales (Table 2).

Table 2 shows that on the five time scales, AR has positive correlations with both AAT and AP at a high significance level of 0.01. In another words, although the runoff, temperature and precipitation displayed nonlinear variations, the runoff presented a linear correlation with the temperature and precipitation. In addition, both of the statistic F and coefficient of determination R^2 for each regression equation showed an increasing trend with the time scale. This pattern indicated that the impact of AAT

Table 1 Basic parameters of the BPANN for hydro-climatic process at different time scales

Time scale	Neuron number of the hidden layer	Input variables	Output variables	Transfer function	Train function	Best epoch	Average absolute error/$10^8 m^3$	Average relative error
S1	4	AAT, AP	AR	tansig	trainlm	4	2.3163	6.65%
S2	4	AAT, AP	AR	tansig	trainlm	5	1.4335	4.25%
S3	4	AAT, AP	AR	tansig	trainlm	6	0.9905	2.85%
S4	4	AAT, AP	AR	tansig	trainlm	6	0.1938	0.57%
S5	4	AAT, AP	AR	tansig	trainlm	10	0.0617	0.18%

Notes: AR - annual runoff, AAT - annual average temperature, and AP - annual precipitation; S1, S2, S3, S4, and S5 represent 2-year, 4-year, 8-year, 16-year, and 32-year time scales, respectively. "tansig" is the hyperbolic tangent sigmoid transfer function, and "trainlm" is a network training function that updates weight and bias values according to Levenberg-Marquardt optimization.

Table 2 MLREs for hydro-climatic process at different time scales

Time scale	Regression equation	R^2	F	Average absolute error/$10^8 m^3$	Average relative error
S1	$AR = 2.251AAT + 0.036AP + 34.420$	0.541	28.932	2.9997	8.41%
S2	$AR = 4.098AAT – 0.002AP + 52.921$	0.745	71.584	1.9987	5.85%
S3	$AR = 2.922AAT + 0.048AP + 34.263$	0.917	269.877	0.9714	2.69%
S4	$AR = 5.644AAT + 0.010AP + 56.036$	0.978	1066.793	0.4501	1.26%
S5	$AR = 5.216AAT – 0.009AP + 59.490$	0.999	30814.085	0.0779	0.22%

Notes: Significance level = 0.01; AR - annual runoff, AAT - annual average temperature, and AP - annual precipitation; S1, S2, S3, S4 and S5 represent 2-year, 4-year, 8-year, 16-year and 32-year time scales, respectively.

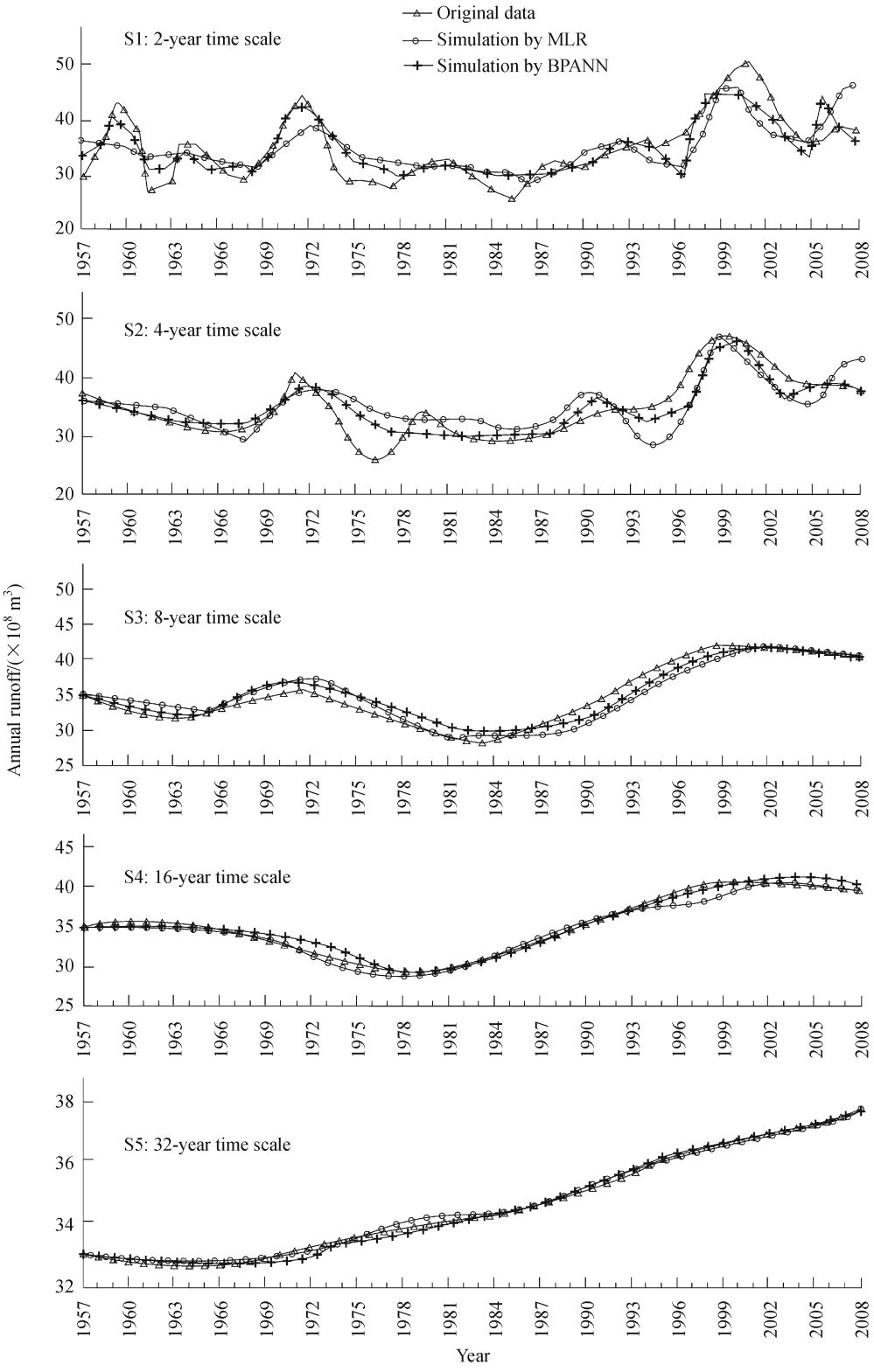

Fig. 5 Simulated results for AR by BPANN and MLR at the different time scales

Table 3 Comparison between BPANN and MLR model at different time scales

Time scale		S1	S2	S3	S4	S5
MLRE	Coefficient of determination	0.541	0.556	0.916	0.977	0.978
	AIC	143.347	102.296	24.869	−63.774	−248.01
BPANN	Coefficient of determination	0.715	0.856	0.920	0.998	0.999
	AIC	118.4882	72.50646	22.28173	−151.494	−259.208

and AP on AR is more significant at a larger time scale than at a smaller time scale.

Table 2 also shows that, the simulated error of MLR is large at the time scale of S1 and S2 (i.e., 2-year and 4-year scale), moderate at the time scale of S3 (i.e., 8-year scale), and small at the time scale of S4 and S5 (i.e., 4-year and 5-year scale).

The coefficient of determination and AIC value in Table 3 also indicate that the MLRE is the best at time scale of S5, and the worst at time scale of S1.

4.3.2 Comparison between BPANN and MLR

Figure 5 reveals the original data of AR, and the simulated values by MLR and BPANN at different time scales, respectively.

Table 3 shows the coefficient of determination as well as the AIC value for BPANN and MLRE at each time scale.

A higher coefficient of determination and a lower AIC value indicate a better model. Overall, comparing the two modeling methods above, i.e., the MLR and BPANN based on WA, we conclude that the BPANN is better than the MLR at each time scale. In other words, both MLR and BPANN successfully simulated the hydro-climatic process based on WA, but the effect from BPANN is better than that from MLR.

5 Discussion and conclusions

Many studies indicate that the hydro-climatic process is a complex system with nonlinearity, but it is difficult to understand the mechanism of hydro-climatic process thoroughly (Xu et al., 2013). The results of this study show that the simulated effect at a larger time scale is better than that at a smaller time scale, and the estimated precision at a larger time scale is higher than that at a smaller time scale.

Our study also reveals that the hydro-climatic process at a large time scale (e.g., 32-year scale) is basically a linear process, but at a small time scale (e.g., 2-year or 4-year scale) it is essentially a nonlinear process with complicated causations. Therefore, the estimated precision is high at a large time scale (e.g., 32-year scale) because the time series of runoff are monotonically related to long-term climatic changes. However, it is difficult to accurately predict a nonlinear hydro-climatic process at a small time scale (e.g., 2-year or 4-year scale).

Nevertheless, our method of combining BPANN and WA provides an approach to understand the hydro-climatic process of Kaidu River from a multi-scale perspective. The approach can be used to explore the hydro-climatic process of other inland rivers in northwestern China.

The main conclusions of this work can be summarized as follows:

(i) The variation of runoff was a response to the regional climate change. In the past five decades, the AR was mainly affected by AAT and AP.

(ii) The variation patterns of temperature and precipitation were scale-dependent in time. Different time scales resulted in the different patterns of AAT and AP. At the time scale of S5, i.e., 32-year scale, AR presented a monotonically increasing trend with AAT and AP. But at the time scale of S1, S2, S3, and S4, i.e., 2-year, 4-year, 8-year, and 16-year scale, AR presented nonlinear variation with fluctuations of AAT and AP.

(iii) The relationship between AR with AAT and AP was successfully simulated by the MLR as well as the BPANN based on WA at each time scale, but the simulated effect from BPANN is better than that from MLR.

Acknowledgements This work was supported by the National Basic Research Program of China (No. 2010CB951003), the Director Fund of the Key Laboratory of GIScience of the Ministry of Education, China, and Projects of West Light Foundation of the Chinese Academy of Sciences (Nos. XBBS201008 and XBBS201026).

References

Anderson D R, Burnham K P, Thompson W L (2000). Null hypothesis testing: problems, prevalence, and an alternative. J Wildl Manage, 64 (4): 912–923

Banakar A, Azeem M F (2008). Artificial wavelet neuro-fuzzy model based on parallel wavelet network and neural network. Soft Comput, 12(8): 789–808

Bruce L M, Koger C H, Li J (2002). Dimensionality reduction of hyperspectral data using discrete wavelet transform feature extraction. IEEE Trans Geosci Rem Sens, 40(10): 2331–2338

Burnham K P, Anderson D R (2002). Model Selection and Multimodel Inference: a Practical Information—Theoretic Approach (2nd Edition). New York: Springer-Verlag

Cannon A J, McKendry I G (2002). A graphical sensitivity analysis for statistical climate models: application to Indian monsoon rainfall

prediction by artificial neural networks and multiple linear regression models. Int J Climatol, 22(13): 1687–1708

Chen J, Kumar P (2004). A modeling study of the ENSO influence on the terrestrial energy profile in North America. J Clim, 17(8): 1657–1670

Chen Y N, Takeuchi K, Xu C C, Chen Y P, Xu Z X (2006). Regional climate change and its effects on river runoff in the Tarim Basin, China. Hydrol Processes, 20(10): 2207–2216

Chen Y N, Xu C C, Hao X M, Li W H, Chen Y P, Zhu C G, Ye Z X (2009). Fifty-year climate change and its effect on annual runoff in the Tarim River Basin, China. Quat Int, 208(1–2): 53–61

Chen Y N, Xu Z X (2005). Plausible impact of global climate change on water resources in the Tarim River Basin. Sci China Ser D-Earth Science, 48(1): 65–73

Chen Z S, Chen Y N, Li B F (2012). Quantifying the effects of climate variability and human activities on runoff for Kaidu River Basin in arid region of northwest China. Theor Appl Climatol, DOI: 10.1007/s00704-012-0680-4

Chou C M (2007). Efficient nonlinear modeling of rainfall-runoff process using wavelet compression. J Hydrol (Amst), 332(3–4): 442–455

Dorofki M, Elshafie A H, Jaafar O, Karim O A, Mastura S (2012). Comparison of artificial neural network transfer functions abilities to simulate extreme runoff data. International Proceedings of Chemical, Biological and Environmental Engineering, 33: 39–44

Farge M (1992). Wavelet transforms and their applications to turbulence. Annu Rev Fluid Mech, 24(1): 395–458

Gan T Y (2000). Reducing vulnerability of water resources of Canadian Prairies to potential droughts and possible climate warming. Water Resour Manage, 14(2): 111–135

Hao X M, Chen Y N, Xu C C, Li W H (2008). Impacts of climate change and human activities on the surface runoff in the Tarim River Basin over the last fifty years. Water Resour Manage, 22(9): 1159–1171

Hsu K, Gupta H V, Sorooshian S (1995). Artificial neural network modeling of the rainfall-runoff process. Water Resour Res, 31(10): 2517–2530

Kermani B G, Schiffman S S, Nagle H G (2005). Performance of the Levenberg–Marquardt neural network training method in electronic nose applications. Sens Actuators B Chem, 110(1): 13–22

Labat D (2005). Recent advances in wavelet analyses: Part 1. A review of concepts. J Hydrol (Amst), 314(1–4): 275–288

Maier H R, Dandy G C (1998). The effect of internal parameters and geometry on the performance of back-propagation neural networks: an empirical study. Environ Model Softw, 13(2): 193–209

Mallat S G (1989). A theory for multiresolution signal decomposition: the wavelet representation. IEEE Trans Pattern Anal Mach Intell, 11 (7): 674–693

Moghadassi A R, Parvizian F, Hosseini S M, Fazlali A R (2009). A new approach for estimation of PVT properties of pure gases based on artificial neural network model. Braz J Chem Eng, 26(1): 199–206

Ramsey J B (1999). Regression over timescale decompositions: a sampling analysis of distributional properties. Econ Syst Res, 11(2): 163–184

Shao Q X, Wong H, Li M, Ip W C (2009). Streamflow forecasting using functional-coefficient time series model with periodic variation. J Hydrol (Amst), 368(1–4): 88–95

Shi Y F, Shen Y P, Kang E S, Li D L, Ding Y J, Zhang G W, Hu R J (2007). Recent and future climate change in northwest china. Clim Change, 80(3–4): 379–393

Smith L C, Turcotte D L, Isacks B L (1998). Streamflow characterization and feature detection using a discrete wavelet transform. Hydrol Processes, 12(2): 233–249

Sun G M, Dong X Y, Xu G D (2006). Tumor tissue identification based on gene expression data using DWT feature extraction and PNN classifier. Neurocomputing, 69(4–6): 387–402

Tao H, Wang G Y, Shao C, Song Y D, Zhou S P (2007). Climate change and its effects on runoff at the headwater of Kaidu River. Journal of Glaciology and Geocryology, 29(3): 413–417 (in Chinese with English abstract)

Torrence C, Compo G P (1998). A practical guide to wavelet analysis. Bull Am Meteorol Soc, 79(1): 61–78

Wang J, Li H, Hao X (2010). Responses of snowmelt runoff to climatic change in an inland river basin, northwestern China, over the past 50 years. Hydrol Earth Syst Sci, 14(10): 1979–1987

Xu J H (2002). Mathematical Methods in Contemporary Geography. Beijing: Higher Education Press (in Chinese)

Xu J H, Chen Y N, Ji M H, Lu F (2008b). Climate change and its effects on runoff of Kaidu River, Xinjiang, China: a multiple time-scale analysis. Chin Geogr Sci, 18(4): 331–339

Xu J H, Chen Y N, Li W H, Dong S (2008a). Long-term trend and fractal of annual runoff process in mainstream of Tarim River. Chin Geogr Sci, 18(1): 77–84

Xu J H, Chen Y N, Li W H, Ji M H, Dong S (2009a). The complex nonlinear systems with fractal as well as chaotic dynamics of annual runoff processes in the three headwaters of the Tarim River. J Geogr Sci, 19(1): 25–35

Xu J H, Chen Y N, Li W H, Ji M H, Dong S, Hong Y L (2009b). Wavelet analysis and nonparametric test for climate change in Tarim River Basin of Xinjiang during 1959–2006. Chin Geogr Sci, 19(4): 306–313

Xu J H, Chen Y N, Li W H, Nie Q, Hong Y L, Yang Y (2013). The nonlinear hydro-climatic process in the Yarkand River, northwestern China. Stochastic Environ Res Risk Assess, 27(2): 389–399

Xu J H, Chen Y N, Li W H, Yang Y, Hong Y L (2011b). An integrated statistical approach to identify the nonlinear trend of runoff in the Hotan River and its relation with climatic factors. Stochastic Environ Res Risk Assess, 25(2): 223–233

Xu J H, Chen Y N, Lu F, Li W H, Zhang L J, Hong Y L (2011a). The nonlinear trend of runoff and its response to climate change in the Aksu River, western China. Int J Climatol, 31(5): 687–695

Xu J H, Li W H, Ji M H, Lu F, Dong S (2010). A comprehensive approach to characterization of the nonlinearity of runoff in the headwaters of the Tarim River, western China. Hydrol Processes, 24 (2): 136–146

Xu J H, Lu Y, Su F L, Ai N S (2004). R/S and wavelet analysis on the evolutionary process of regional economic disparity in China during the past 50 years. Chin Geogr Sci, 14(3): 193–201

Zhang Q, Xu C Y, Tao H, Jiang T, Chen D (2010). Climate changes and their impacts on water resources in the arid regions: a case study of the Tarim River basin, China. Stochastic Environ Res Risk Assess, 24 (3): 349–358

AUTHOR BIOGRAPHIES

Jianhua Xu obtained his B.S. of mathematics and M.S. of geography from Lanzhou University, China in 1986 and 1988, respectively. He worked as a Professor in Department of Geography at Lanzhou University from 1996 to 2000. Then, he has been working as a Professor in the Key Lab of GIScience of the Education Ministry of China, East China Normal University until now. He has hosted and finished more than 30 research projects which from National Natural Science Fund of China, National Social Science Fund of China, as well as from the support of provinces and ministries of China. He has already published 13 books and more than 100 academic papers. His research interests focus on geographical modelling, GIS and remote sensing application. E-mail: jhxu@geo.ecnu.edu.cn

Yaning Chen obtained his B.S. and Ph.D. from Department of Geology, Northwest University, China in 1982 and 2000, respectively. Now, he is a Professor of Xinjiang Institute of Ecology and Geography, Chinese Academy of Sciences, and the Director of the State Key Laboratory of Oasis Ecology and Desert Environment. He has hosted and finished more than 40 research projects which from National Natural Science Fund of China, National Basic Research Program of China, as well as from the support of provinces and ministries of China. He has already published more than 100 academic papers. His research interests focus on climate change and hydrology in arid area. E-mail: chenyn@ms.xjb.ac.cn